KN Scattering and the Nucleon Strangeness Radius

M. J. Ramsey-Musolf[1,3] and H.-W. Hammer[1,2,*]

[1]*Institute for Nuclear Theory, University of Washington, Seattle, Washington 98195*
[2]*Universität Mainz, Institute für Kernphysik, D-55099 Mainz, Germany*
[3]*Department of Physics, University of Connecticut, Storrs, Connecticut 06269*

(Received 23 May 1997)

The leading nonzero electric moment of the nucleon strange-quark vector current is the mean square strangeness radius $\langle r_s^2 \rangle$. We evaluate the lightest Okubo-Zweig-Iizuka–allowed contribution to $\langle r_s^2 \rangle$, arising from the kaon cloud, using dispersion relations. Drawing upon unitarity constraints as well as K^+N scattering and $e^+e^- \to K\overline{K}$ cross section data, we find the structure of this contribution differs significantly from that suggested by a variety of QCD-inspired model calculations. In particular, we find evidence for a strong ϕ-meson resonance which may enhance the scale of kaon cloud contribution to an observable level. [S0031-9007(98)05552-5]

PACS numbers: 14.20.Dh, 11.55.Fv, 12.39.Jh, 13.75.Jz

The reasons for the success of the nonrelativistic quark model (NRQM) in accounting for the static properties of low-lying hadrons remains one of the unsolved mysteries of nonperturbative QCD. It has been postulated that—as far as low-energy observables are concerned—constituent quarks of the NRQM effectively account for the QCD degrees of freedom inside hadrons [1]. This suggestion may be tested, in part, by measuring observables which depend only on the sea quarks and gluons, such as the matrix element $\langle N|\overline{s}\gamma_\mu s|N\rangle$. By now there exists a well-defined program of parity-violating (PV) electron-nucleus scattering experiments dedicated to the determination of this matrix element [2]. The theoretical understanding of this matrix element is much less clear. To date, only two results from the lattice have been reported [3], and they appear to conflict with the recent results for the strangeness magnetic form factor reported by the SAMPLE Collaboration [4]. The use of hadronic effective theory, in the guise of chiral perturbation theory, is also limited, as chiral symmetry does not afford an independent determination of the relevant low-energy constants [5]. A third alternative—the use of QCD-inspired models—is equally problematic, and model predictions for the mean square strangeness radius $\langle r_s^2 \rangle$ and magnetic moment μ_s vary considerably in magnitude and sign (for a recent review of model calculations, see Ref. [5]).

In this Letter, we analyze the strangeness radius using a fourth approach, namely, dispersion relations (DR's). Our objective is to identify the hadronic mechanisms which govern the leading strangeness moments without relying on QCD-inspired nucleon models. To that end, we focus on the lightest Okubo-Zweig-Iizuko (OZI)-allowed contribution, which arises from the so-called "kaon cloud" or $K\overline{K}$ intermediate state. A variety of model calculations reported to date have assumed that (a) OZI-allowed processes, in the guise of virtual strange intermediate states, give the most important contributions to the leading strangeness moments; and (b) these processes are adequately described by truncating at second order in the strong hadronic couplings, g. In the case of $\langle r_s^2 \rangle$, the resultant predictions are generally smaller than would be observable in the parity-violating electron scattering experiments. Moreover, kaon cloud predictions are typically an order of magnitude smaller than those obtained with DR's under the assumption of vector meson dominance (VMD), which relies on the extraction of a large ϕNN coupling from analyses of the isoscalar electromagnetic (EM) form factors [6]. Assumption (a) has been analyzed elsewhere and shown to be questionable [7]. Regarding assumption (b), we find that the structure of the strangeness form factors differs significantly from the assumptions underlying kaon cloud models, particularly the validity of the second-order approximation. Using the kaon cloud as an illustrative case study, we show that the scale of OZI-allowed contributions depends critically on effects going beyond $\mathcal{O}(g^2)$, and that a proper inclusion of such effects may enhance the scale of OZI-allowed contributions to an experimentally detectable level. We also demonstrate the relationship between resonance [6] and kaon cloud contributions, resolving a long-standing issue in this field.

Of the form factors which parametrize $\langle N|\overline{s}\gamma_\mu s|N\rangle$, we focus on the strangeness electric form factor $G_E^{(s)}$, for which we obtain our most reliable results. Since $G_E^{(s)}$ vanishes at $q^2 = 0$, we write a subtracted dispersion relation for this form factor and its leading, nonvanishing moment:

$$G_E^{(s)}(t) = \frac{t}{\pi} \int_{t_0}^{\infty} dt' \, \frac{\mathrm{Im}\, G_E^{(s)}(t')}{t'(t' - t)}, \tag{1}$$

$$\langle r_s^2 \rangle = 6 \, \frac{dG_E^{(s)}}{dt} \bigg|_{t=0} = \frac{6}{\pi} \int_{t_0}^{\infty} dt' \, \frac{\mathrm{Im}\, G_E^{(s)}(t')}{t'^2}, \tag{2}$$

where $t = q^2$ and t_0 begins a cut along the real t axis associated with a given physical intermediate state. The state having the lowest threshold t_0 is the 3π state, whose

contribution is nominally OZI violating. The lightest OZI-allowed contribution arises from the $K\overline{K}$ state, for which $t_0 = 4m_K^2$. Following the analysis of Ref. [8], we express the $K\overline{K}$ contribution to the absorptive part of the electric form factor as a product of the appropriate $K\overline{K} \to N\overline{N}$ partial wave and the kaon strangeness vector current form factor:

$$\mathrm{Im}\, G_E^{(s)}(t) = \mathrm{Re}\left\{\left(\frac{Q}{4m_N}\right) b_1^{1/2,\,1/2}(t) F_K^{(s)}(t)^*\right\}. \quad (3)$$

Here, $Q = \sqrt{t/4 - m_K^2}$, $F_K^{(s)}$ parametrizes the matrix element $\langle 0|\bar{s}\gamma_\mu s|K(k_1)\overline{K}(k_2)\rangle$, and $b_1^{\lambda,\lambda'}$ is the $J = 1$ partial wave for $K\overline{K}$ to scatter to the state $|N(\lambda)\overline{N}(\lambda')\rangle$ with λ, λ' denoting the corresponding helicities.

The problem now is to determine $b_1^{1/2,\,1/2}$ and $F_K^{(s)}$ as reliably as possible. For $t \geq 4m_N^2$, the physical $N\overline{N}$ production threshold, one may in principle use $K\overline{K} \to N\overline{N}$ data to determine the scattering amplitude. Alternatively, we note that in this kinematic region, the unitarity of the S matrix implies that $|b_1^{\lambda,\lambda'}| \leq 1$ [8]. Given the present quality of $K\overline{K} \to N\overline{N}$ scattering data, it turns out to be more effective to insert the unitarity bound on $b_1^{1/2,\,1/2}$ into Eq. (3). The corresponding bound on the contribution from $t \geq 4m_N^2$ to the dispersion integral of Eq. (2) is negligible (see Table I).

To evaluate $b_1^{1/2,\,1/2}$ in the unphysical region $4m_K^2 \leq t \leq 4m_N^2$, one must rely on some method of analytic continuation. The $\mathcal{O}(g^2)$ (one-loop) model calculations of $G_E^{(s)}$ implicity rely on an analytic expression to effect this continuation. The one kaon-loop approximation is equivalent to using a DR in which the $b_1^{\lambda,\lambda'}$ are computed in the Born approximation (BA) and the kaon strangeness form factor taken to be pointlike $[F_K^{(s)}(t) \equiv -1]$ [8]. The BA calculation yields an analytic expression for $b_1^{1/2,\,1/2}$, which may be analytically continued to unphysical values of t. When computed in this approximation, however, the $b_1^{\lambda,\lambda'}$ violate the unitarity bound by a factor of 4 or more for $t \geq 4m_N^2$ [8]. This violation reflects the omission of important kaon rescattering and other short-distance hadronic mechanisms which render the scattering amplitude consistent with the requirements of unitarity. Given the magnitude of the unitarity violation at the physical threshold, one would infer that the BA represents a rather drastic approximation in the unphysical region and that truncation at $\mathcal{O}(g^2)$ is questionable.

TABLE I. Kaon cloud prediction for $\langle r_s^2\rangle$ for the two scenarios discussed in the text. Second and third columns give contributions to the dispersion integral of Eq. (2) from integration regions corresponding to unphysical (second column) and physical (third column) t-channel scattering amplitudes. In both scenarios, the unitarity bound on $b_1^{1/2,\,1/2}$ is imposed for $t \geq 4m_N^2$.

Moment	Scenario	$4m_K^2 \leq t \leq 4m_N^2$	$4m_N^2 \leq t$	Total
$\langle r_s^2\rangle$ [fm^2]	$\mathcal{O}(g^2)$	-0.017	-0.007	-0.024
$\lvert\langle r_s^2\rangle\rvert$ [fm^2]	AC/GS	0.065	0.001	0.066

An alternate strategy, which we follow here, is to perform a fit to experimental K^+N scattering amplitudes and analytically continue the results for the fit into the unphysical region. The success of this approach depends on the quality of the data, the kinematic range over which it exists, and the stability of the fit. It is advantageous to consider K^+N (s-channel) amplitudes, since the analytic continuation may be performed without encountering problematic singularities occurring in the u-channel reaction K^-N. As experimental input, we use the recent phase shift analysis of the VPI group [9]. The requisite K^+N amplitudes of sufficient quality exists over the range $-8m_K^2 \lesssim t < 0$. We correspondingly expect our continuation to yield a credible estimate of the scattering amplitude for $0 \leq t \lesssim 8m_K^2$. Although this range does not include the entire unphysical region over which one must compute the dispersion integral, it is sufficiently broad for our present purposes. Indeed, the structure we find in the continued amplitude in this region appreciably affects the kaon cloud contribution to $\langle r_s^2\rangle$.

We carry out the continuation by using backward dispersion relations. This method relies on the coincidence of s- and t-channel amplitudes in the kinematic domain: $\cos\theta_s = \cos\theta_t = -1$ for a given value of t, where θ_s and θ_t are the c.m. scattering angles. Thus, we may continue the s-channel amplitude to the unphysical region in t, and equate this amplitude with the corresponding t-channel amplitude: $A(\cos\theta_s = -1, t_{\mathrm{phys}}) \to A(\cos\theta_s = -1, t_{\mathrm{unphys}}) = A(\cos\theta_t = -1, t_{\mathrm{unphys}})$. In performing the continuation of the backward s-channel amplitude, we follow conventional procedures [10,11] and work with the discrepancy function, ΔA:

$$\Delta A(t) = A(t) - A^{\mathrm{pole}}(t) - \frac{\mathcal{P}}{\pi}\int_0^{t_p} dt' \frac{\mathrm{Im}\, A^{\mathrm{exp}}(t')}{t' - t} - \frac{1}{\pi}\int_{t_p}^{-\infty} dt' \frac{\mathrm{Im}\, A^{\mathrm{model}}(t')}{t' - t}, \quad (4)$$

where data exist in the range $t_p \leq t \leq 0$, $A^{\mathrm{exp}}(t)$ gives the experimental amplitude in this range, $A^{\mathrm{model}}(t)$ gives a model for the high-energy part of the amplitude, and $A^{\mathrm{pole}}(t)$ denotes the Λ, Σ pole terms, which are known exactly (the dependence on $\cos\theta_s$ is implicit). The function ΔA is analytic for real values of t in the range $t_p \leq t \leq 0$, whereas the full amplitude has a cut in this region. For A^{model}, we use a Regge exchange model fit [12]. The inferred high-t behavior is $A^{\mathrm{model}}(t) \propto |t|^\alpha$, with $\alpha = -1.2$, and the constant factor is determined from the highest-energy experimental point.

The continuation proceeds by replacing $A(t) \to \mathrm{Re}\, A^{\mathrm{exp}}(t)$ in Eq. (4) and performing a fit to the experimental values for ΔA in the range $t_p \leq t \leq 0$. This

fit is most easily accomplished by first carrying out a conformal map $t \to z(t)$, transforming the domain of analyticity for ΔA into a circle of unit radius [13]. A convergent expansion of the amplitude is then made using Legendre polynomials, $P_k(z)$, and the coefficients determined from a fit to the experimental values for ΔA. In practice, we fit $g(z(t)) = \Delta A/|t|^{\alpha}$, which divides out the high energy behavior of ΔA and improves the stability of the continuation. The discrepancy function—and, via Eq. (4), the full backward amplitude—is then obtained in the unphysical region by evaluating the Legendre expansion for $z = z(t_{\rm unphys})$.

The final step in obtaining $b_1^{1/2,\,1/2}$ is to expand $A(\cos\theta_t = -1, t_{\rm unphys})$ in partial waves, using the helicity basis as in Refs. [8,11]. Since the amplitude is known only for one value of θ_t, a separation of the $b_1^{\lambda,\lambda'}$ from the $b_{J\neq 1}^{\lambda,\lambda'}$ relies on several additional observations: (a) The only significant enhancements of the $J \geq 2$ partial waves occur via resonances, (b) the lightest $J > 1$, $I = 0$ resonance having a non-negligible branching ratio to the $K\overline{K}$ state is the $f_2(1270)$, whose mass lies near the upper end of the range in $\sqrt{t}$ for which we expect our continuation to be valid, and (c) the use of a realistic parametrization for $F_K^{(s)}$ in Eq. (3) dramatically suppresses contributions for $\sqrt{t} \gtrsim 1.4$ GeV/c. We thus expect little contamination from the $f_2(1270)$ and higher-lying resonances in the region near the $K\overline{K}$ threshold, which gives the dominant contribution to $\langle r_s^2\rangle$, and we correspondingly omit the $J \geq 2$ partial waves.

The remaining $J = 0$ and $J = 1$ partial waves may be separated by drawing on the work of Refs. [11,14]. In those analyses, the strength and approximate peak position of the $J = 0$ partial wave were determined from KN phase shift analyses using backward dispersion relations and its generalization.

As a check on our general procedure, we reproduce the results of Ref. [10] for the πN case. Furthermore, we have tested the sensitivity of our results for $\langle r_s^2\rangle$ to changes of the high-energy parameter α and the truncation point of the fitted Legendre series, n. We find that the structure of the continued amplitudes and resultant value of $\langle r_s^2\rangle$ change by $\lesssim 15\%$ as α and n are varied over reasonable ranges. We obtain the results shown in Fig. 1 and Table I using $n = 6$ and the value for α taken from the Regge model fit [12], $\alpha = -1.2$.

The results of this analysis are displayed in Fig. 1(a), where we plot the kaon cloud contribution to the spectral function for $\langle r_s^2\rangle$ as a function of t. We give the spectral function computed using a pointlike form factor (PFF) for $F_K^{(s)}$ and two scenarios for $b_1^{1/2,\,1/2}$: (I) the BA, and (II) analytic continuation (AC) of K^+N scattering amplitudes. We also show the upper limit on the spectral function generated by the unitarity bound on $b_1^{1/2,\,1/2}$ for $t \geq 4m_N^2$. The curve obtained in scenario (II) contains a peak in the vicinity of the $\phi(1020)$ meson, presumably reflecting

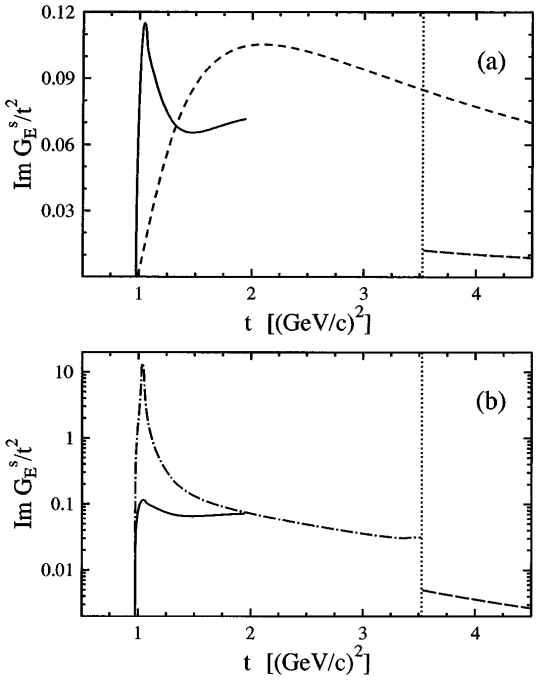

FIG. 1. $K\overline{K}$ contribution to the spectral function for $\langle r_s^2\rangle$ in units of $(\mathrm{GeV}/c)^{-4}$. Short-dashed curve (a) gives results for $\mathcal{O}(g^2)$ calculation. Solid curve [(a),(b)] gives AC/PFF results, while long-dashed curves show unitarity bound for $t \geq 4m_N^2$ using PFF (a) and GS form factor (b). Dash-dotted curve gives AC/GS spectral function (b). Dotted vertical line indicates physical $N\overline{N}$ production threshold.

the presence of a $K\overline{K} \leftrightarrow \phi$ resonance in the scattering amplitude. This structure enhances the spectral function over the result obtained at $\mathcal{O}(g^2)$ near the beginning of the $K\overline{K}$ cut. As t increases from $4m_K^2$, the spectral function obtained in scenario (II) falls below that of scenario (I), ostensibly due to $K\overline{K}$ rescattering which must eventually bring the spectral function below the unitarity bound for $t \geq 4m_N^2$. As observed previously in Ref. [8], and as illustrated in Fig. 1(a), the $\mathcal{O}(g^2)$ approximation omits these rescattering corrections and consequently violates the unitarity bound by a factor of 4 or more even at threshold.

Turning to the kaon strangeness form factor, we note that the assumption of pointlike behavior $[F_K^{(s)}(t) \equiv -1]$ is poorly justified on phenomenological grounds. Data for $e^+e^- \to K\overline{K}$ indicate that the kaon EM form factor is strongly peaked for $t \approx m_\phi^2$ and falls off sharply from unity for $t \gtrsim 2$ $(\mathrm{GeV}/c)^2$. Although there exist no data for $F_K^{(s)}(t)$, one expects it to behave in an analogous fashion to $F_K^{EM}(t)$ [8]. We therefore follow Ref. [8] and employ a Gounaris-Sakurai (GS) parametrization for $F_K^{(s)}$, which produces the correct normalization at $t = 0$ and a peak in the vicinity of the ϕ meson. The corresponding spectral function is shown in Fig. 1(b), where comparison is made with the spectral function computed using a pointlike $F_K^{(s)}$. The use of

the GS parametrization significantly enhances the spectral function near the beginning of the $K\overline{K}$ cut as compared with the pointlike case, while it suppresses the spectral function for $t \gtrsim 2\ (\mathrm{GeV}/c)^2$. We note that other parametrizations for $F_K^{(s)}$, such as a simple ϕ-dominance form, yield similar results for the spectral function.

The numerical consequences of using experimental K^+N amplitudes to determine $b_1^{1/2,\,1/2}$ and of employing a realistic kaon strangeness form factor are indicated in Table I. The first line gives the $\mathcal{O}(g^2)$ kaon cloud prediction for $\langle r_w^2 \rangle$, using a pointlike $F_K^{(s)}$ and $b_1^{1/2,\,1/2}$ computed in the BA. The second line gives results when the GS form factor and analytically continued fit to K^+N amplitudes for $b_1^{1/2,\,1/2}$ are used (AC/GS). In both cases the unitarity bound on $b_1^{1/2,\,1/2}$ is imposed for $t \geq 4m_N^2$. The AC/GS results were obtained by extending $b_1^{1/2,\,1/2}$ to $4m_N^2$. Although we believe the continuation to be trustworthy only for $t \lesssim 8m_K^2$, and although the continued $b_1^{1/2,\,1/2}$ amplitude exceeds the unitarity bound for $t \to 4m_N^2$, the GS form factor suppresses contributions for $t \geq 8m_K^2$, rendering the overall contribution from $8m_K^2 \leq t \leq 4m_N^2$ negligible. Since we are presently unable to determine the relative phases of $F_K^{(s)}$ and $b_1^{1/2,\,1/2}$ as a function of t, the AC/GS results represent an upper bound on $|\langle r_s^2 \rangle|$ and carry an uncertain overall sign [8]. Hence, we give only the magnitude in Table I.

With these caveats in mind, we observe that the use of a realistic, nonperturbative $K\overline{K}$ spectral function increases the kaon cloud contribution to $\langle r_s^2 \rangle$ by roughly a factor of 3 as compared to the $\mathcal{O}(g^2)$ calculation. Moreover, the nonperturbative result approaches the scale at which the PV electron scattering experiments are sensitive, whereas the $\mathcal{O}(g^2)$ prediction is too small to be seen. The enhanced scale of the kaon cloud depends critically on the presence of the resonance structure near $t = m_\phi^2$ in *both* $b_1^{1/2,\,1/2}$ and $F_K^{(s)}$ (Fig. 1). This structure—obtained without relying on the *a priori* assumption of pole dominance in $G_E^{(s)}$ or $G_E^{I=0}$—demonstrates how the resonance contribution arises out of the $K\overline{K}$ continuum and yields a kaon cloud result similar in magnitude to pure VMD predictions [6].

Although the kaon cloud is only one of the virtual hadronic states through which $s\overline{s}$ pairs may contribute to the strangeness form factors, our result illustrates the importance of including effects to all orders in g when computing any of these hadronic contributions. In particular, we speculate that the results of the NRQM calculation reported in Ref. [15], which includes contributions from a tower of OZI-allowed intermediate states, will be significantly modified when effects beyond $\mathcal{O}(g^2)$ are included. Our analysis suggests that these effects, in the guise of resonant and nonresonant meson rescattering, determine the structure and scale of OZI-allowed contributions. The presently available scattering data are not likely to afford a model-independent, all-orders treatment of higher-mass contributions. Nevertheless, any model estimate of the higher-mass content of $s\overline{s}$ spectral functions must be evaluated by comparing its kaon cloud prediction with the results of the analysis reported here.

We gratefully acknowledge useful discussions with D. Drechsel, G. Höhler, N. Isgur, and R. L. Jaffe. This work has been supported in part by the Deutsche Forschungsgemeinschaft (SFB 201) and the German Academic Exchange Service (Doktorandenstipendien HSP 111) (H. W. H.) and in part under U.S. Department of Energy Contract No. DE-FG06-90ER40561 and a National Science Foundation Young Investigator Award (M. J. R.-M.).

*Present address: TRIUMF, 4004 Wesbrook Mall, Vancouver, BC, Canada V6T 2A3.

[1] D. B. Kaplan and A. Manohar, Nucl. Phys. **B310**, 527 (1988).
[2] M. J. Musolf *et al.*, Phys. Rep. **239**, 1 (1994), and references therein.
[3] D. B. Leinweber, Phys. Rev. D **53**, 5115 (1996); S. J. Dong, K. F. Liu, and A. G. Williams, hep-ph/9712483.
[4] SAMPLE Collaboration, B. Mueller *et al.*, Phys. Rev. Lett. **78**, 3824 (1997).
[5] M. J. Ramsey-Musolf and H. Ito, Phys. Rev. C **55**, 3066 (1997).
[6] R. L. Jaffe, Phys. Lett. B **229**, 275 (1989); see also H.-W. Hammer, U.-G. Meißner, and D. Drechsel, Phys. Lett. B **367**, 323 (1996).
[7] H.-W. Hammer and M. J. Ramsey-Musolf, Phys. Lett. B **416**, 5 (1998).
[8] M. J. Musolf, H.-W. Hammer, and D. Drechsel, Phys. Rev. D **55**, 2741 (1997).
[9] J. S. Hyslop *et al.*, Phys. Rev. D **46**, 961 (1992).
[10] H. Nielsen, J. Lyng Peterson, and E. Pietarinen, Nucl. Phys. **B22**, 525 (1970).
[11] H. Nielsen and G. C. Oades, Nucl. Phys. **B41**, 525 (1972).
[12] V. Barger, Phys. Rev. **179**, 1371 (1969).
[13] N. M. Queen and G. Violini, *Dispersion Theory in High-Energy Physics* (Wiley, New York, 1975), Chap. 12.
[14] R. A. W. Bradford and B. R. Martin, Z. Phys. C **1**, 357 (1979).
[15] P. Geiger and N. Isgur, Phys. Rev. D **55**, 299 (1997).